

# Analysis of Magnetic Flux Linkage Distribution in Salient-Pole Synchronous Generator with Different Kinds of Inter-Turn Winding Faults

H. Yaghobi\*, K. Ansari\*\* and H. Rajabi Mashhadi\*\*

**Abstract:** A reliable and accurate diagnosis of inter-turn short circuit faults is a challenging issue in the area of fault diagnosis of electrical machines. The purpose of this study is to present a more efficient technique in fault detection and to provide a reliable method with low-cost sensors and simple numerical algorithms which not only detects the occurrence of the fault, but also locates its position in the winding. Hence, this paper presents a novel method for diagnosis of different kinds of inter-turn winding faults in a salient-pole synchronous generator based on changes in the magnetic flux linkage. It describes the influence of inter-turn winding faults on the magnetic flux distribution of the generator. The main feature of the proposed method is its capability to identify the faulty coils under two types of inter-turn winding faults. Also, the occurrence of two other types of faults can be detected by the proposed technique. Simple algorithm, low cost sensor and sensitivity are the other features of the proposed technique. Experimental results derived from a 4-pole, 380V, 1500 rpm, 50 Hz, 50 KVA, 3-phase salient-pole synchronous generator confirm the validity of the proposed method.

**Keywords:** Synchronous Generator, Fault Diagnosis, Linkage Flux Analysis, Inter-turn Winding Fault.

## 1 Introduction

The stator's internal short circuit current in the synchronous generator may be several times larger than its terminal short circuit current [1]. When an inter-turn short circuit occurs, the shorted turn will act as the secondary winding of an autotransformer. Consequently, a very large circulating current will flow in the faulted turn. This circulating current creates excessive heat and high magnetic forces in the machine [2]. Therefore, it is very important to have a careful analysis of the internal faults in synchronous generators to increase their useful life and reliability. Hence a reliable and accurate diagnosis of inter-turn short circuit faults is a challenging problem in the area of fault diagnosis of electrical machines. The expertise in this field is still in permanent evolution and new methods appear every year [3]. The purpose of this study is to be more efficient in fault detection and to provide a reliable

method with low-cost sensors and simple numerical algorithms [3] which not only detects the occurrence of the fault, but also locates its position in the winding.

However, the behavior of the synchronous machine under internal faults has not been thoroughly studied [4], and few methods exist for analyzing internal faults in synchronous machines [1], [4], [5], [8]-[14]. Most of these methods are based on the mathematical, two reaction theory and winding function approach. Two reaction theory is derived from the assumption that the machine windings are symmetrical. When an internal fault occurs on the stator winding of a synchronous machine, it divides the faulty winding into a number of sections and the symmetry between these faulted sections and the rest of the machine windings will lose. Therefore, the models based on the two-reaction theory cannot be useful to analyze internal faults [5]. Usually, mathematical methods do not consider the saturation effects or consider the saturation effects in synchronous machines with the dqo analysis which uses the superposition principle to solve for the d-axis path and the q-axis path separately. However, superposition is not valid in modeling saturation effects due to the nonlinearity of the saturation phenomena [6], [7]. In a salient pole synchronous machine, the air gap is

---

Iranian Journal of Electrical & Electronic Engineering, 2011.

Paper first received 14 Nov. 2010 and in revised form 25 Jun. 2011.

\* The Author is with the Department of Engineering, Sari Branch, Islamic Azad University, Sari, Iran.

E-mail: h.yaghobi@iausari.ac.ir

\*\* The Authors are with the Department of Electrical Engineering, Ferdowsi University of Mashhad, Iran.

E-mail: h\_mashhadi@um.ac.ir

nonuniform and the reluctance of the magnetic flux path is a function of time. Therefore the magnetic fluxes along the d-axis and the q-axis are varying and the level of saturation along these two axes is also changeable [7]. The methods presented in [1], [5], [8]-[13] do not consider the saturation inside the machine.

Reference [4] has investigated the effects of turn-to-earth fault on the synchronous machine inductances by the winding function approach. In this method, the magnetic hysteresis, slotted stator effects and the saturation effect are not taken into account for the sake of simplification [4]. In the Symmetrical Components Method used in [10], only the fundamental and the third harmonic components of time and space are considered. This leads to a substantial amount of error, since internal faults give rise to increased harmonic content [1], [8], [11]. In the multiloop method that is proposed in [8] and [9], a salient-pole synchronous machine is considered as made of several electric circuits, each composed of the actual loops that are formed by the coils. The inaccuracies and complexity in the calculation of loop inductances prevents the generalization of this model to diverse types of synchronous machine, especially for machines with many coils in the stator and rotor [1], [4], [11].

In [1], one of the parallel paths is divided into two parts, whose magnetic axis locations have the invariability. Indeed, the magnetic axis should locate where each fundamental component obtains the maximum value [11]. References [11]-[13] present a winding partitioning technique for solving the internal fault problem in sinusoidal wound machines. Such windings are scarcely found in electrical machines; hence, the application of this method is also limited.

On the other hand, it has now become vital to diagnose faults at their very inception; as unscheduled machine downtime can cause heavy financial losses [14]. Hence, as a recent trend, monitoring techniques for electrical machines has been considered very important [15]. Condition monitoring of synchronous generators could prevent tragic losses and prepare precise view of machine operation. It must be noted that a variety of factors need to be considered when selecting the most suitable monitoring method for application in an industrial environment. The most important factors are presented in [16]. It is very difficult and, in most cases, impossible to gratify all the criteria, mainly because of the complexity of the degradation mechanisms, abnormalities, and the nature of the fault [16].

Fault monitoring of rotating electrical machines using magnetic field measurements have been proposed as a topical subject of investigation [3], [17]. The leakage flux detection has been introduced as an efficient technique for diagnosis. In this method leakage flux sensor is located outside the machine. This method has been used for the detection of stator winding short-circuit [18]-[22]. Unfortunately, the efficiency of this

method has not yet been pointed out since it is related to the signal processing used for harmonic detection [3].

In this paper, we present a novel method for the diagnosis of different kinds of inter-turn winding faults in a salient-pole synchronous generator using the change in the magnetic flux linkage. The main feature of the proposed method is that it is capable of identifying the faulty coils under two types of inter-turn winding faults. Also, occurrence of two other types of faults can be detected by the proposed technique. Simple algorithm, low cost sensor and sensitivity are other features characterized the proposed technique. In this method, the generator air gap flux linkage is measured via search coils sensor installed under the stator wedges inside the machine. This sensor is readily accessible on the market and its cost is very low.

## 2 Description of the Inter-Turn Winding Faults

Early stages of internal faults in stator winding may often have insignificant effects on the machine performance; however such faults may quickly lead to considerable inter-turn faults and subsequently destructive failures [23]. Four kinds of internal faults in stator winding are stator turn-to-turn short circuit in the same branch, turn-to-turn short circuit of two branches in the same phase, turn-to-turn short circuit of two branches in different phases, and turn-to-earth fault are presented in Fig. 1 [8].

Undetected turn-to-turn faults lead to generated heat in the deformed region of a winding which finally grows and is changed into phase-to-ground or phase-to-phase faults [24]. This type of faults is a major reason of the stator winding failures and other faults may be result from this fault [24]. In addition, a severe fault such as a phase-to-ground fault may lead to irreversible damage to the stator winding and core [23]. Therefore, it is very important to analyze and detect stator inter-turn faults at an early stage to prevent further damage to the machine and involved systems. In this section, an internal turn-to-turn short circuit in the same branch is discussed and simulated. However, this discussion and simulation can be extended to cover all kinds of internal faults.

### 2.1 MMF Distortion Due to the Fault

Figure 1 (b) illustrates the case when a turn-to-turn short circuit has happened in the same branch between two points, m and n. Also Fig. 1 (b) shows that two currents produce opposite MMFs, one of which is the

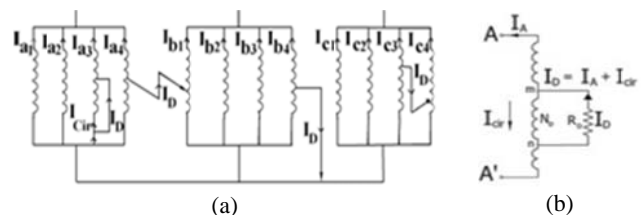


Fig. 1 (a) Four kinds of internal faults [8]. (b) Inter-turn short circuit between two points, m and n [16].

phase current and the other one is the short circuit current (The difference between these two currents is defined as circulating current  $I_{cir}$ ). Therefore, the main effect of the inter-turn short circuits decreases the MMF close to the short-circuited turns [16]. Under ideal conditions, the machine has an air-gap magneto-motive force which varies sinusoidally in space and time. In this condition, the air-gap MMF function  $M$  is the sum of the field and the armature winding MMF:

$$M = M_f + M_{ABC} \quad (1)$$

The field winding MMF is defined by the equation:

$$M_f = N_f I_f M_{fn} \quad (2)$$

where  $N_f$  denotes the number of field winding turns per pole and  $I_f$  is the field current. The function  $M_{fn}$  denotes a unitary trapezoid function given by:

$$M_{fn} = \frac{4}{\pi} \frac{1}{\gamma_f} \sum_{n=1,3,5,\dots} \frac{\sin \gamma_f}{n^2} \sin(n \frac{p}{2} (\theta_m - w_m t)) \quad (3)$$

$\theta_m$  denotes the mechanical angular coordinate in a stator fixed reference frame.  $t$  is the time and  $p$  is the pole number.  $\gamma_f$  is the angle between the height and lateral side of the trapezoid function  $M_{fn}$ . Also, the three-phase armature MMF can be expressed as [25]:

$$M_{N_{ph},ABC} = i_a \cdot \sum_{n=1,3,5,\dots} \hat{M}_n \sin(n \frac{p}{2} \theta_m) + i_b \cdot \sum_{n=1,3,5,\dots} \hat{M}_n \sin((n \frac{p}{2} (\theta_m - \frac{4\pi}{3p})) + i_c \cdot \sum_{n=1,3,5,\dots} \hat{M}_n \sin((n \frac{p}{2} (\theta_m + \frac{4\pi}{3p})) \quad (4)$$

where  $i_a$ ,  $i_b$ , and  $i_c$  denote the currents in the winding phases A, B, and C respectively. The coefficients  $\hat{M}_n$  are given by:

$$\hat{M}_n = \frac{4}{\pi} \frac{N_{ph}}{p} \frac{1}{n} k_d(n) k_p(n) k_{sl}(n) \quad (5)$$

where  $N_{ph}$  denotes the total number of winding turns per phase circuit. Expressions for the distribution, pitch and slot opening factors (symbols  $k_d(n)$ ,  $k_p(n)$ , and  $k_{sl}(n)$  respectively), can be found in [26].

Now, consider a turn-to-turn short circuit in the same branch on stator winding in phase A. During fault generator operation, the MMF function can be accordingly expressed as follows:

$$M = M_f + M_{(N_{ph}-N_D),A} + M_{N_{ph},B,C} - M_{ND} \quad (6)$$

where  $M_{(N_{ph}-N_D),A}$  denotes the armature winding MMF of the faulty phase A. In fact, when a short circuit occurs, the number of phase winding turns and the MMF produced by this winding reduce. This MMF can be expressed as follows:

$$M_{(N_{ph}-N_D),A} = i_a \cdot \sum_{n=1,3,5,\dots} \hat{M}_n \sin(n \frac{p}{2} \theta_m), \quad (7)$$

$$\hat{M}_n = \frac{4}{\pi} \frac{N_{ph} - N_D}{p} \frac{1}{n} k_d(n) k_p(n) k_{sl}(n)$$

$N_D$  corresponds to the winding turns being short. Also,  $M_{N_{ph},B,C}$  denotes the armature winding MMF of the healthy phase B, C and can be expressed as follows:

$$M_{N_{ph},B,C} = i_b \cdot \sum_{n=1,3,5,\dots} \hat{M}_n \sin((n \frac{p}{2} (\theta_m - \frac{4\pi}{3p})) + i_c \cdot \sum_{n=1,3,5,\dots} \hat{M}_n \sin((n \frac{p}{2} (\theta_m + \frac{4\pi}{3p})) \quad (8)$$

During the fault, the coefficients  $\hat{M}_n$  in these phases are not changed and are given by Eq. (5).

$M_{ND}$  denotes the MMF produced by the short-circuit current is contrary to the MMF produced by phase winding and can be expressed as follows:

$$M_{ND,sc} = N_D \times i_D \quad (9)$$

On the other hand, the amplitude of the fault current,  $i_D$ , depends on the fault resistance,  $R_D$ , and the induced voltage,  $v_{sc}$ , in the shorted coil. Hence,  $i_D$  can be expressed as follows [27]:

$$i_D = \frac{v_{sc}}{R_D} \quad (10)$$

In addition, for frequencies lower than 10 kHz, the voltage gradient from turn to turn is constant and therefore the voltage is approximately distributed uniformly across the turns of the phase winding. Moreover, for a winding factor, approximately equal to one, the voltage in the shorted turns can be expressed as follows [27]:

$$v_{sc} = (\frac{N_D}{N_{ph}}) v_{ph} \quad (11)$$

This induced voltage,  $v_{sc}$ , correspondingly depends on the number of shorted turns,  $N_D$ , that is associated with this short portion of the faulty phase winding in the machine.  $N_{ph}$  is the effective number of turns of the phase winding and  $v_{ph}$  is the phase voltage. Hence, the fault current can be stated as follows:

$$i_D = (\frac{v_{ph}}{R_D}) (\frac{N_D}{N_{ph}}) \quad (12)$$

Consequently, faulty operation will cause a distortion in the air-gap magneto-motive force of the machine.

## 2.2 Magnetic Flux Distribution

Modeling and analysis of salient-pole synchronous generator is very complicated, especially when an inter-turn winding fault occurs in a generator equipped with a stator winding consisting of parallel branches. In many

applications, a 2-D finite element analysis gives relatively precise prediction of the magnetic field distribution and machine performance. Some limitations of 2-D analysis imply that the use of 3-D analysis is inevitable if an accurate analysis is needed. These limitations are presented in [28]. In this research, in order to improve the overall accuracy, the magnetic field distribution is calculated by 3D-FEM using ANSYS workbench software. In modeling of the salient-pole synchronous generator, saliency and slotting, magnetic saturation effects, and the position of the winding inside the stator are included in the FEM modeling. Slotting and the position of the winding can be seen in Fig. 2(a). In order to prevent confusion, only excitation and phase A windings are shown in Fig. 2(a). Also, the effect of magnetic saturation was included in the FEM software by using B-H curves of the rotor and stator cores. When an internal fault is on the stator winding, the fault winding is divided into some sub coils. In order to model this using FEM, the ampere-turns distribution for the windings should be represented in the model. It is necessary to consider the short circuited turns separately in the FEM model when confronting with the  $N_D$  turns missing from the phase winding due to the internal fault. The current source  $I_{cir} = I_D - I_A$  is inserted into short circuited turns (see Fig. 1(b)). This current is in opposite direction with the phase current. Fig. 2(b) shows the short circuit fault model [29].

Figure 3 (a) and (b) shows the typical magnetic flux distribution under normal and turn-to-turn fault of the studied generator as obtained by the FEM simulation. In Fig. 3(a) magnetic flux distribution varies from 0.177 T (q-axis) to 1.503 T (d-axis). Fig. 3(b) illustrates flux distribution under turn-to-turn fault. In this figure, magnetic flux distribution varies from 0.195 T to 1.654 T. Due to the high circulating current in the fault areas; magnitude of magnetic flux linkage under fault condition in these areas is higher (also, see Fig. 6). It is evident from both figures that magnetic field distribution in synchronous generator under healthy operation is symmetrical. But when a turn-to-turn fault occurs, this fault will cause nonsymmetrical distribution of magnetic flux linkage. Also, this matter will be shown in section 5 by experiments (see Figs. 10 and 11). Therefore, magnetic field distribution could be applied for detection of the turn-to-turn faults in synchronous generator. In fact, in electrical machines, air-gap magnetic field distribution in no-load and on-load performance under healthy conditions is symmetrical (neglecting the insignificant inherent asymmetry in the magnetic field distribution due to the differences on mechanical structures). But this symmetry is specially lost under internal faults occurrence.

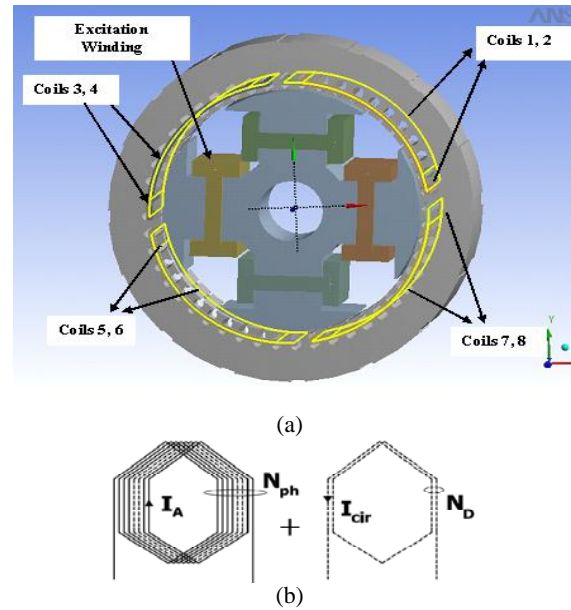


**Fig. 2** (a) Positions of the phase A conductors inside the stator in the FEM modeling. (b) Short circuit fault model [29].

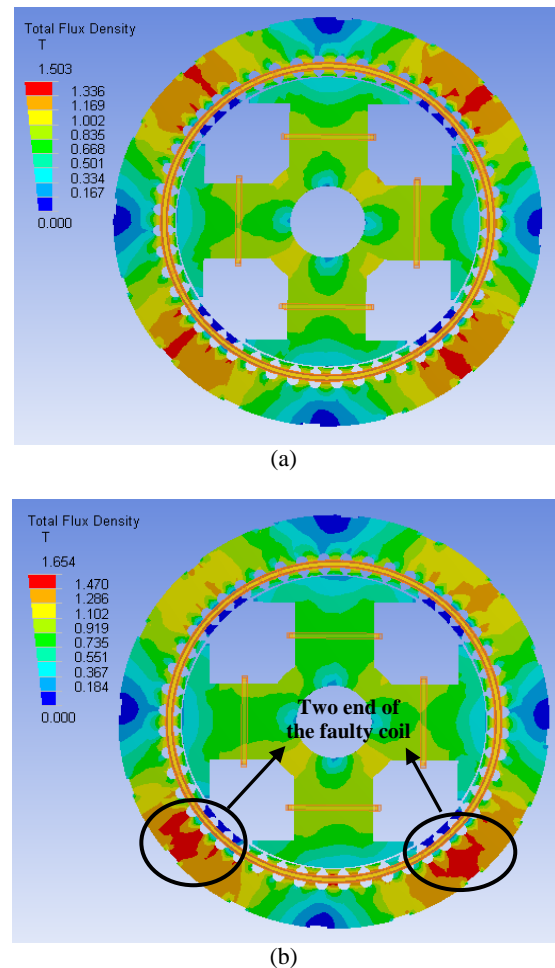


**Fig. 3** Distribution of magnetic field density in salient-pole synchronous generator (front view). (a) Under healthy condition. (b) Under turn-to-turn short circuit in stator winding.

### 3 Experimental Test Setup and Measuring Technique

To demonstrate the performance of presented method, a series of actual different kinds of inter-turn winding fault on a salient-pole synchronous generator have been fulfilled. It will be shown, when an inter-turn winding fault occurs, the fault will cause considerable changes on the magnetic flux linkage. Therefore magnetic flux linkage is a suitable criterion for diagnosis of inter-turn winding faults.

#### 3.1 Experimental Test Setup

The machine used in this study is a 50 KVA, 380V, 4-pole, 1500 rpm, 50 Hz, 48 stator slots, salient-pole synchronous generator. The stator of this generator has a 3-phase, one layer, lap winding, and four parallel branches in each phase. The structure of the testing laboratory and experimental test setup is shown in Fig. 4.

It consists of a synchronous generator connected to a three-phase load. This generator has no damper winding, and is driven by an induction machine. In fact, a usual commercially accessible generator was disassembled and in order to produce turn-to-turn fault, isolation of the few turns from the some coil was scratched. At these points some conductors were soldered and taken them out of the machine Short circuit was made between these conductors. Thus, turns were shorted externally. By measuring EMF between these conductors and having awareness of winding details, we were capable to deduce how many turns in one coil were shorted. In this work, the minimum number of turn of the stator winding are being short circuited is approximately about 5% of the total turn number. A no-load experiment and a three-phase symmetrical terminal short-circuit experiment are accomplished on the machine without internal faults. Next, several of internal faults were performed on the mentioned generator under different conditions. In these experiments, any resistor to limit the currents is not used. Also, in order to prevent severe damage to the generator, the duration of the inter-turn short circuit was limited by using a switch. Measurements at full excitation current were carried out under normal condition. However, because of the major concern about test machine health for further tests, measurements at full excitation current were not carried out under fault condition.

Through the experiments performed in this work, search coils and designed electronic-microcontroller board are used for measuring simultaneously flux linkage data in cross-section of the aforementioned generator. Designed electronic-microcontroller board has one master and forty eight slaves. Serial port interface has been used for connecting designed electronic-microcontroller board to computer. The induced voltages in the search coils are communicated to serial port of the computer by means of designed

electronic-microcontroller board. Schematic and experiment view of these used search coils are illustrated in Fig. 5.

#### 3.2 Measurement of the Machine Flux Linkage with Search Coil

The search coil sensor is widely used for flux measurement in electrical machine [30]. But there is a natural reluctance to place a search coil if it could possibly hazard the machine or personnel. There seems little doubt that suitable search coils could be placed at the machines, as the hazards can be made insignificant. It worth mentioning that, these sensors are now becoming common on large generators and have now been installed in a large number of generators in the Central Electricity Generating Board [31].

The theory behind the search-coil sensor is Faraday's law of induction and induced voltage in the search coils is directly proportional to the rate of change of the flux. Search coil sensors can sense magnetic fields as weak as  $2 \times 10^{-5}$  nT. Also, there is no upper limit to their sensitivity range [30]. These inductive sensors observe the real distribution of the air-gap flux density. This indicates that all the damping effects produced by the saturation and the parallel current branches of the stator winding are taken into account. This sensor is readily accessible on the market and its cost is very low in comparison with the capacitive air-gap monitoring system. Easiness and the low price of the used inductive sensors allow the installation of a high number of sensors [32]. Hence, in order to improve the accuracy, in this research, forty eight single turn search coils were installed along the grooves of the stator teeth with a pitch of  $15^\circ$  with the aim of being able to determine how the flux linkage distribution in the generator changes when an abnormal operational condition is present. Also, this sensor has more advantages such as insensitivity to external conditions (humidity, temperature, etc.), no need to mechanical disassembling / reassembling, and easiness to remove.

#### 4 Different Operation Conditions and Loading Effect

The induced voltage in the sensors under different operation conditions and loading effect are explained in this section. Figure 6 (a) and (b) shows the measured voltage induced in a search coil, under healthy and faulty operations at no-load, respectively. Under ideal conditions, the machine has an air-gap magnetic field which varies sinusoidally in space and time. Faulty operation will cause a distortion of this sinusoidal waveform. Due to the high circulating current in the fault areas; magnitude of magnetic flux linkage under fault condition in these areas is higher. Also, Fig. 6(c) and (d) shows the simulation stator teeth voltage at steady state condition under healthy and faulty operations at no-load. Good agreement is obtained between the measured and simulated waveforms.



Fig. 4 Testing laboratory and experimental test setup.

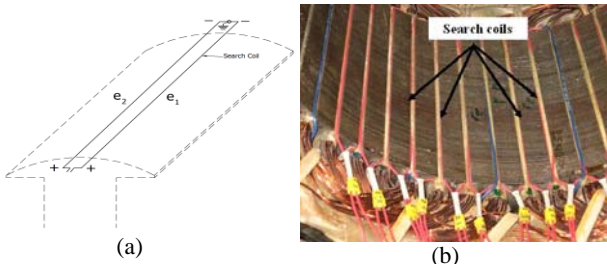


Fig. 5 (a) Schematic view of search coil. (b) Search coils placed along the stator teeth in experiment.

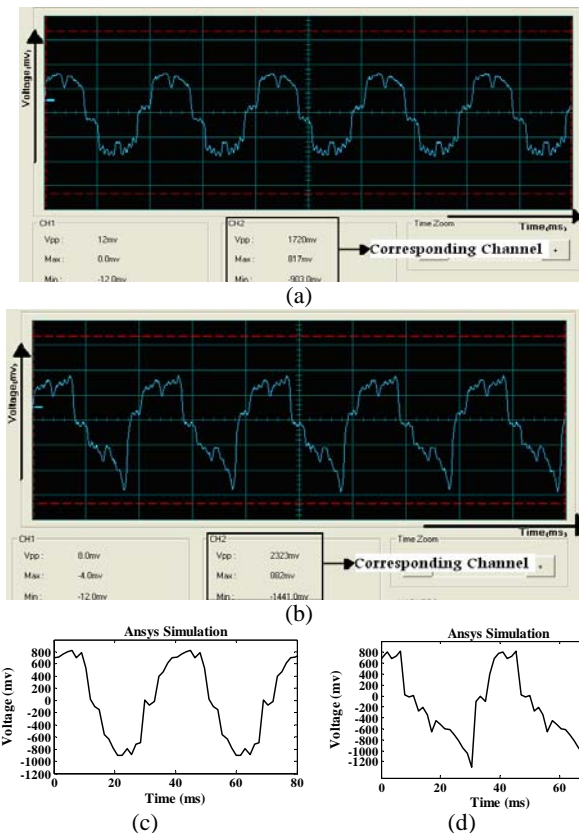
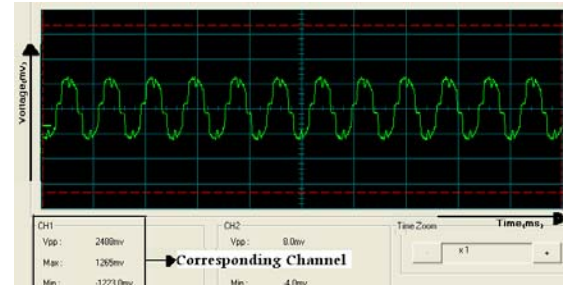
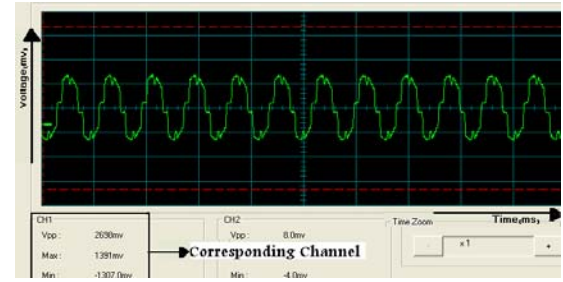


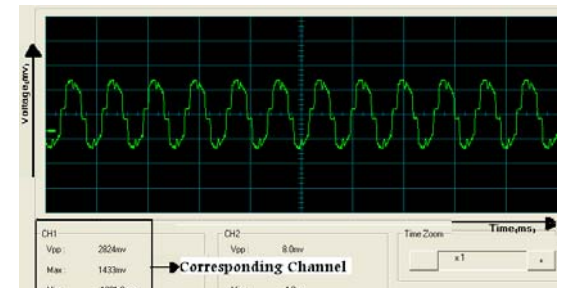
Fig. 6 Measured and simulated voltage (no-load). (a) Measured voltage under healthy operation. (b) Measured voltage under faulty operation. (c) Simulated voltage under healthy operation. (d) Simulated voltage under faulty operation.



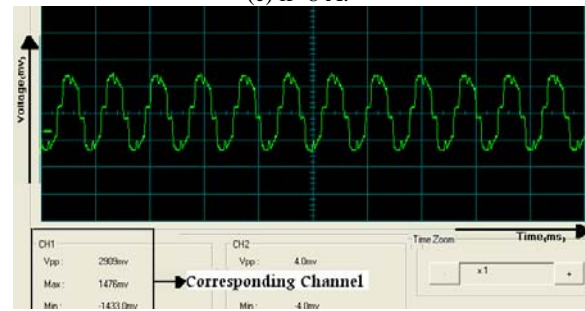
(a)  $i_f=4$  A.



(b)  $i_f=6$  A.



(c)  $i_f=8$  A.



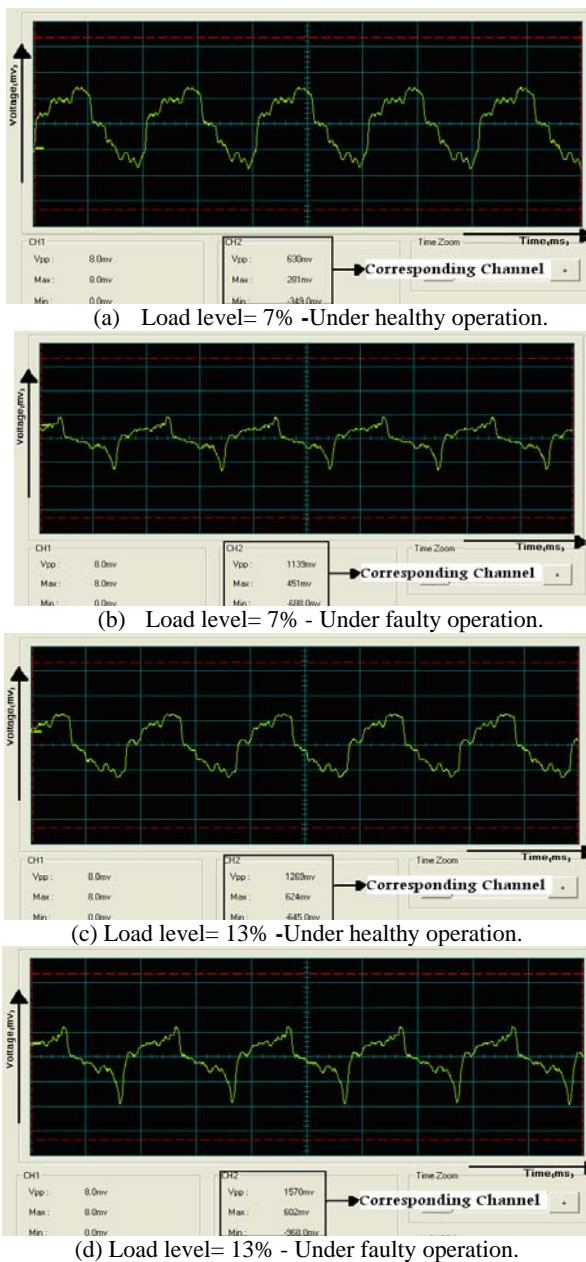
(d)  $i_f=9.8$  A.

Fig. 7 Measured induced voltage in a search coil under different excitation current in the normal operations.

Figure 7 illustrates the no load voltage induced in a search coil, as the rotor current increases with no fault present in experiment. A field current of 9.8 A represents extreme saturation. According to this figure, the different saturation level will affect the magnitude of the induced voltage in search coils proportional to machine no-load curve. In fact when the rotor current increases, nature of the induce voltage in a search coil at different saturation level is stable and does not a substantial change.

On the other hand, due to limitation in the power of the induction machine, generator has been loaded up to a

maximum of around 25% of the rated load. Although influence of load level on the detection procedure might seem a drawback, experimental tests showed it is possible to make a reliable diagnosis. Fig. 8 shows induced voltages in a search coil, under different on-load conditions in the normal and faulty operations. As it is seen in this figure, the generator load level does not have a major influence on the performance levels of the method. According to Figs.6, and 8, due to the effect of the armature reaction, under on-load conditions, induced voltages in the search coils slightly deviate from the induced voltages in the search coils under no-load conditions.



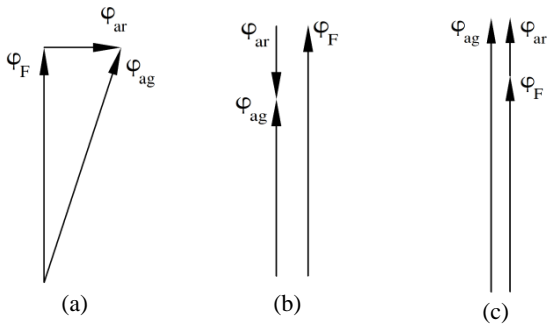
**Fig. 8** Induced voltage in the 31<sup>st</sup> search coil under different on-load conditions in the normal and faulty operations.

Figure 9 indicates how the armature reaction affects the rotor-produced flux ( $\phi_r$ ) for three power factor (PF) conditions: unity, leading, and lagging. In this figure  $\phi_{ar}$  is stator produced flux and  $\phi_{ag}$  is the resultant magnetic flux that rotates at synchronous speed. It is evident from this figure, that unity power factor condition (resistive load) gives maximum deviation under normal operation [33]. In fact, in a p poles, healthy, symmetrical machine, the magnetic axis of each pole is located at  $360/p$  geometrical degrees [34]. Under load conditions, the pole axis is not an axis of symmetry whereas in no-load conditions the pole axis is axis of symmetry. When a generator is delivering power to the load, the axes of symmetry of the magnetic field deviates from the polar and interpolar axes [35].

### 5 Effect of Different Kinds of Inter-Turn Winding Faults on Magnetic Flux Linkage

As far as the authors are aware, most of the presented techniques do not offer the capability of identifying the specific faulty coil [1], [4], [5], [8]-[13]. In addition, in most these techniques only one type of fault was investigated. On the other hand, as discussed in [27], in lap winding machine not only faulty coil can not be detected, but also finding the faulty phase is too difficult. In lap wound machines, the electrical space phase shift between the magnetic axis of the faulty coil and the original magnetic axis of the phase winding depends on the location of the shorted coil, the number of coils per phase and the distribution of the coils in the stator slots. Consequently, it is difficult to detect the faulty phase in these types of machines [27]. In addition, finding a clear fault signatures in a machine equipped with the stator winding configurations of the parallel branches in internal faults is a difficult task [16]. On the other hand, along with the growth of electric power industry, investigation of fault diagnosis of synchronous generators with several parallel paths becomes more and more significant [1].

Although the stator of studied generator in this paper has lap winding and four parallel branches in each phase, the proposed technique could identify the faulty coils under two types of inter turn winding faults, i.e., turn-to-turn short circuit in the same branch and turn-to-turn short circuit of two branches in same phase. Moreover, in the other two types of faults the proposed technique can specify only the occurrence of faults. In the following subsections, the effect of different kinds of inter-turn winding faults on magnetic flux linkage of the above mentioned generator is presented. To demonstrate the performance of presented method, a series of actual different kinds of inter-turn winding fault on the aforementioned generator have been fulfilled. As representative examples of the many tests performed on the salient-pole synchronous generator in the laboratory, one illustration for each case is presented.



**Fig. 9** Armature reaction for different power factor. (a) PF=1. (b) PF lagging. (c) PF leading [33].

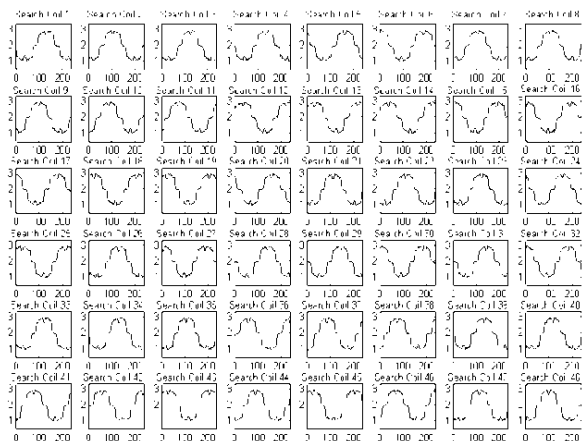


**Fig. 10** Forty eight measured voltage (V) under healthy operation (no-load).

Figure 10 shows the forty eight voltage waveform (induced in the search coils) under no-load condition in the healthy operation. In this figure, symmetry in the magnetic field distribution under healthy operation is presented (also, see Fig. 3(a)). As it was mentioned earlier, under ideal conditions, the machine has an air-gap magnetic field which varies sinusoidally in space and time. Faulty operation will cause a distortion of this sinusoidal waveform.

### 5.1 Turn-to-Turn Short Circuit in the Same Branch and Two Branches in the Same Phase

Turn-to-turn short circuit in the same branch and two branches in the same phase have the same effect on the machine flux linkage. In these two cases because the currents due to the fault will change locally (see Fig. 1(a)), the magnetic flux linkages around the faulty area will be affected by the faults. When the stator winding inter-turn fault occurs, the induced voltages in the search coils of the faulted area change more than those of the other search coils. Because voltage difference and circulating current will occur, the flux linkage in these areas will be most affected with this fault. This concept is shown in Fig. 11(a). To demonstrate this concept, we have created an experimental turn-to-turn fault on the coil between the 21<sup>st</sup> and 31<sup>st</sup> slots in phase W, and the induced voltage in forty eight search coils has been measured.

Figure 11(a) shows the forty eight voltage waveform under no-load condition in the faulty operation. According to this figure, the symmetry in the magnetic field distribution is lost and induced voltage in search coils around two ends of the faulty coil are distorted. Induced voltage in these search coils have more change to induced voltage in other search coils that indicates the fault has occurred in relative coils of them (also, see Fig. 3(b)). Also, similar results were obtained from tests under turn-to-turn short circuit of two branches in the same phase. Fig. 11(b) shows the experiment result of the shorted turns in two branches on the coils between 4<sup>th</sup> and 14<sup>th</sup> slots and 5<sup>th</sup> and 15<sup>th</sup> slots in phase V at 50% (tap to terminal) of branch1 and 75% (tap to terminal) of branch2. According to this figure, it is evident that the symmetry in the magnetic field distribution is lost and induced voltage in search coils around two ends of the faulty coils are distorted. According to Fig. 11(a) and (b), these two types of faults, i.e., turn-to-turn short circuit in the same branch and turn-to-turn short circuit of two branches in the same phase have the same effect on the induced voltage in the search coils. In these faults, the flux linkage adjacent to the faulty coils considerably distorts. The proposed technique can identify the occurrence of these two types of faults as well as faulted coils.

It should be remembered that due to the effect of armature reaction under on-load conditions in the normal and faulty operations, induced voltage in the search coils slightly leave from the induced voltage in the search coils under no-load conditions (see Figs. 6 and 8).

### 5.2 Turn-to-Turn Short Circuit of Two Branches in the Different Phases and Turn-to-Earth Fault

Turn-to-turn short circuits of two branches in different phases and turn-to-earth fault have the same effect on the induced voltage in the search coils. In these two cases because the currents due to the fault will change in all phases (see Fig. 1(a)), the magnetic flux linkages in the all area of the machine will be affected by the fault. Fig. 12(a) and (b) shows the experiment result of the turn-to-earth fault of one path of phase V at 50% under no-load and on-load conditions respectively. According to these figures, induced voltage in all search coils are affected by the fault. In other words, induced voltages in all search coils are distorted.

Also, similar results were obtained from tests under another type of inter-turn winding faults and presented in Fig. 13. Figure 13 shows the experiment result of the shorted turns of two branches in different phases. This fault has been fulfilled in phase V at 50% (tap to terminal) of branch 1 and in phase W at 60% (tap to terminal) of branch 2. According to Figs. 12 and 13, these two types of faults, i.e., turn-to-turn short circuit of two branches in different phases and turn-to-earth fault have the same effect on the machine flux linkages in the machine. In these faults, the flux linkages in the



all space of the machine are affected and considerably distorts. The proposed technique can specify only the occurrence of these two types of faults.

In addition, the rotor unbalance is commonly monitored in electrical machines and as the result, non-uniform flux exist in the air-gap. It must be noted when the rotor is in unbalanced condition, the length of the air-gap changes (see Fig. 14), so it reduces in one side and it increases in another side. Hence, the induced voltage in search coils at areas with less air-gap length will be increased and the induced voltage in search coils at areas with more air-gap length will be decreased.

In fact, the length of the air-gap will affect the magnitude of the induced voltage in search coils. Therefore, under rotor unbalanced conditions, forty eight induced voltages in search coils have different magnitude (under healthy operation, forty eight measured voltages have the same magnitude-see Fig. 10). While in inter-turn winding fault, the length of the air-gap is fixed (see Fig. 14) and the induced voltage in search coils at faulty area will be distorted.

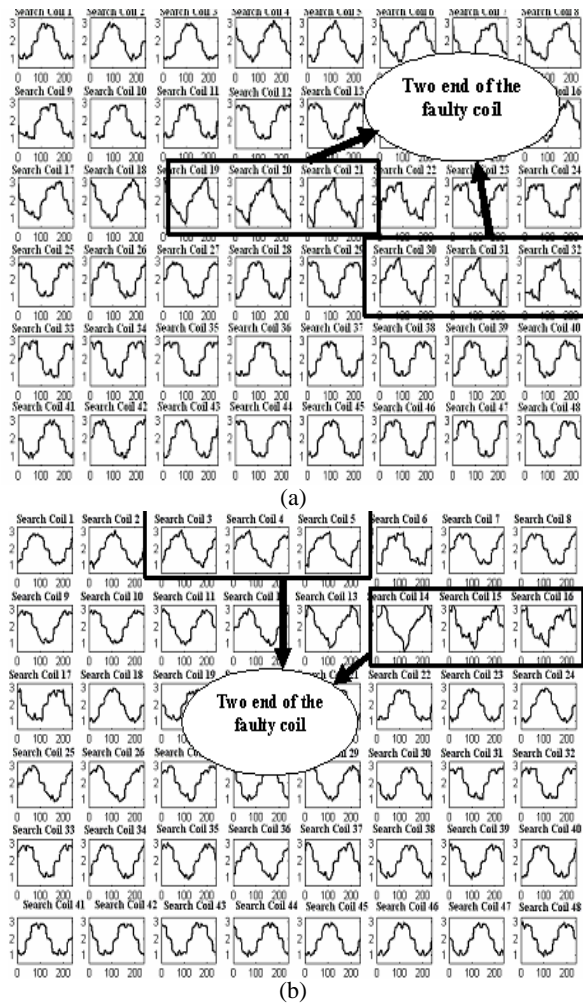


**Fig. 11** (a) Forty eight measured voltage (V) under turn-to-turn short circuit in the same branch in phase W (no-load). (b) Forty eight measured voltage (V) under turn-to-turn short circuit of two branches in the same phase in phase V (no-load).

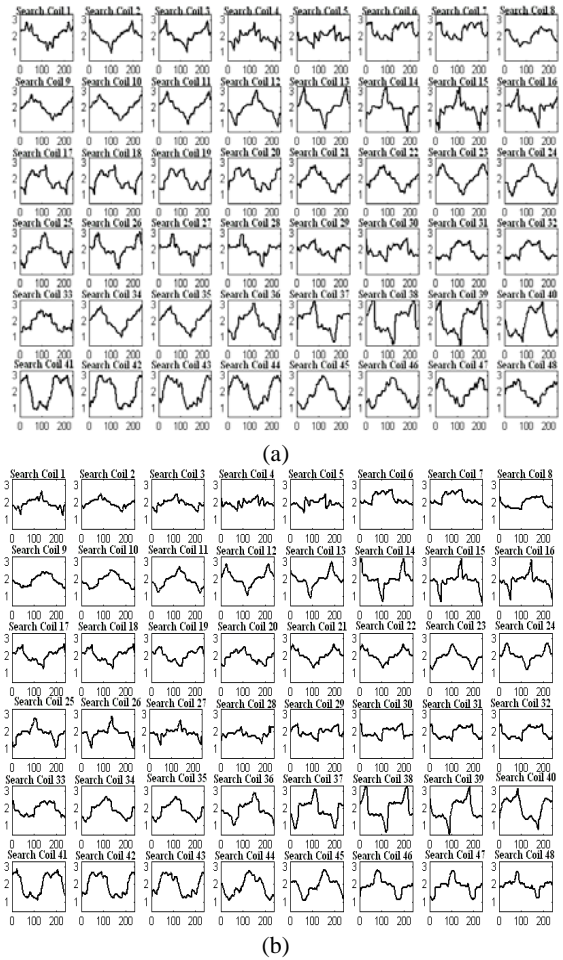


**Fig. 12** Forty eight measured voltage (V) under turn-to-earth fault of one path of phase V at 50% (a) Under no-load condition. (b) Under on-load condition.

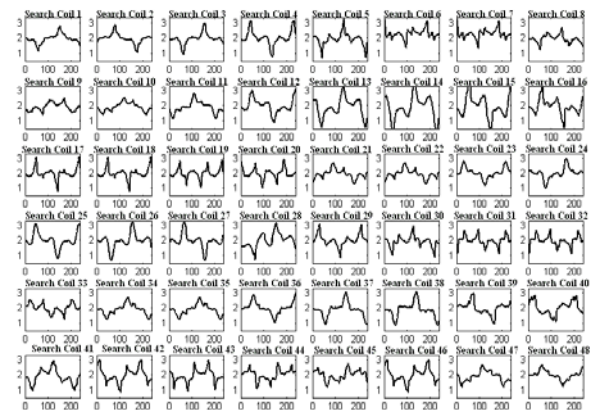


**Fig. 13** Forty eight measured voltage (U) under turn-to-turn short circuit of two branches in different phases in phase V and phase W (on-load).

## 6 Design of Fault Diagnosis System with the Aid of Neural Network

Fault detection of electrical machines has shifted in recent years from conventional techniques to Artificial Intelligence (AI) techniques. AI-based techniques have the potential advantage over the conventional methods

in significantly improving the accuracy in fault detection [36]. In our work, probabilistic neural network (PNN) and discrete wavelet transform (DWT) are used in design of fault diagnosis system. PNN as main part of this fault diagnosis system and DWT are combined effectively to construct the classifier. The PNN is trained by features extracted from the magnetic flux linkage data through the discrete Meyer wavelet transform. PNN is trained with simulation data and then PNN is tested with experimental data. In fact, similar to training section the measured slot flux linkage is preprocessed with wavelet transform and then in order to detect the fault, approximation signal at level 4 is fed to PNN.

### 6.1 Probabilistic Neural Network

PNN is a kind of the Radial Basis Function Neural Networks (RBF's) suitable for classification problems. The PNN networks have some advantages over other artificial neural networks that are presented in the following [37].

- The PNN learns instantaneously in one-pass through the patterns of the training set which causes them faster to train, compared to other networks and these networks don't need pre-decision on the number of layers, hidden units and initial weights.
- The fast learning speed of the PNN makes it suitable for fault diagnosis and signal classification problems in real time (especially when implemented on hardware systems).

### 6.2 Wavelet Decomposition

Many applications use the wavelet decomposition. One of the most popular applications of the wavelet transforms is in de-noising studies on the steady state problems [38]. The aim of de-noising is to eliminate the noise and to retain the important features as much as possible. In this project, DWT is used for de-noising, because by reducing the noise, better network training is done.

### 6.3 Detection of Faulty Coil by MWPNN

In this subsection, procedure for detection of faulty coil by PNN and DWT, based on the previous discussion are presented. Meyer wavelet probabilistic neural network (MWPNN) is utilized to detect the faulty coils. In fact, the basic PNN is integrated with DWT to construct the MWPNN. Forty eight search coils are sampled simultaneously in one or more cycles (depending on the used hardware). Therefore, a vector sets are obtained. The obtained waveforms are analyzed by wavelet transform and de-noised signals are extracted. Then PNN is trained by features extracted from the magnetic flux linkage data through the discrete Meyer wavelet transform. In this scheme, regarding the number of search coils; forty eight MWPNN is used for detection the faulty coils. Each MWPNN is carried out only for two classes i.e., normal and fault for the classification. When no faults are present in the

generator, all MWPNN's will predict the normal class. If some MWPNN's predict the fault class, the turn-to-turn short circuit in the same branch or turn-to-turn short circuit of two branches in the same phase has occurred. Also, if all MWPNN's predict the fault class, the turn-to-turn short circuit of two branches in different phases or turn-to-earth fault has occurred. This process is illustrated in Fig. 15.

Each neural network is trained with 5 input data (or events) of each class. Table 1 lists the parameters of the MWPNN in this procedure for detection of faulty coil. The influence of different kinds of mother wavelets on the classification accuracy was also investigated. It will provide the evidences for choosing proper wavelet family. Five commonly used wavelets, named Meyer wavelet, Haar wavelet, Daubechie's wavelet, Symmlets and Coiflets wavelet are considered. In order to evaluate the performance of different kinds of mother wavelets, we choose the same decomposition level up to 6 levels. The highest classification accuracy is obtained with Meyer wavelet in level 4. Hence, in order to detect the fault, discrete Meyer wavelet transform is used and the approximation signal at level 4 is fed to PNN.

Therefore, MWPNN is used as the supervised classifier. To evaluate the performance of MWPNN, its results are compared with those of different artificial neural networks. These different networks are trained and subsequently tested with the same data due to similar procedure mentioned before. These data for training are obtained from computation with the FEM. Then, the ANN's are tested with the experimental data. These simultaneous data are sampled with those of the designed electronic-microcontroller board from the forty eight search coils in cross-section of the mentioned generator. First, fault diagnosis system uses back-propagation (BP) neural network. Second, system uses PNN and third, system uses MWPNN.

It must be noted that backpropagation neural network is most widespread among all artificial neural networks [39]. These networks are also referred to as multilayered perceptron (MLP) or feedforward networks. The multilayered perceptron neural network is trained with the Batch Gradient Descent with Momentum. In detection of the faulty coil, for the MLP neural network, several network configurations were tried. Better results have been obtained from a network composed of three layers with 240, 24, and 2 neurons. Sigmoid is selected as the act function of neurons in every layer. The results of comparison for the detection of the faulty coil are presented in Table 2.

**Table 1** Parameters of the MWPNN for detection of the faulty coil.

Method	Related parameter	
PNN	Input layer	240 nodes (depending on the used hardware)
	Output layer	2 nodes
	Smoothing parameter	0.5

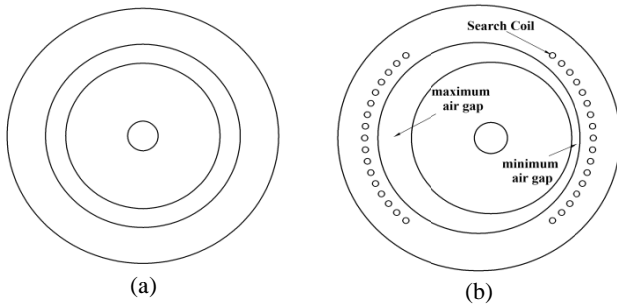


**Fig. 14** Cross-section of machine. (a) Under healthy operation and inter-turn winding fault. (b) Under rotor unbalance condition.

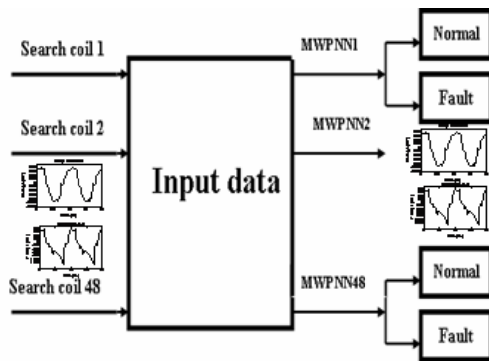


**Fig. 15** Procedure for detection of faulty coil by MWPNN.

**Table 2** Diagnosis accuracy for test results.

ANN	MLP	PNN	MWPNN
Classification accuracy	55%	78%	>95%

## 7 Conclusions

In this paper, the effect of different kinds of inter-turn winding faults on magnetic flux linkage of a salient-pole synchronous generator is presented. The experimental results are obtained to demonstrate the effectiveness of the proposed method. It is shown that the magnetic flux linkage is a suitable criterion for the diagnosis of inter-turn winding faults. The main feature of the proposed method is its capability to identify the faulty coils under two types of inter-turn winding faults. Also, the occurrence of two other types of faults can be detected by the proposed technique. Simple algorithm, low cost sensor and sensitivity are the other features in the proposed technique.

## Acknowledgment

This work is supported by the Mashhad Power Station. The authors are appreciative to Mr. Borzoe for his assistance. Authors wish to thank Mr. Dehnavi, Dr. Hashemian, and Mr. Pordeli in providing the experimental test setup and testing laboratory.

## References

[1] Megahed A. I. and Malik O. P., "Simulation of internal fault in synchronous machines", *IEEE*

*Trans. Energy Convers.*, Vol. 14, No. 4, pp. 1306-1311, Dec.1999.

[2] Stone G. C., Boulter E. A., Culbert I. and Dhirani H., *Electrical Insulation for Rotating Machines*, John Wiley & Sons Publishers: ISBN: 0-471-44506-1, pp.12-20, 2004.

[3] Henao H., Demian C. and Capolino G. A., "A frequency-domain detection of stator winding faults in induction machines using an external flux sensor", *IEEE Transactions on Industry Applications*, Vol. 39, No. 5, pp. 1272-1279, Sept.-Oct. 2003.

[4] Tu X., Dessaint L. A., Kahel M. E. and Barry A. O., "A new model of synchronous machine internal faults based on winding distribution", *IEEE Trans. Ind. Electron.*, Vol. 53, No. 6, pp. 1818-1828, Dec. 2006.

[5] Muthumuni D., McLaren P. G., Dirks E. and Pathirana V., "A synchronous machine model to analyze internal faults", *Industry Applications Conference, 2001. Thirty-Sixth IAS Annual Meeting. Conference Record of the 2001 IEEE*, Vol. 3, pp.1595-1600, 2001.

[6] Cros J., et al. "Simplified design model for fast analysis of large synchronous generators with magnetic saturation", *IEEE International Conference on Electric Machines and Drives*, pp. 1515-1522, 2009.

[7] Marti J. R. and Louie K. W., "A phase-domain synchronous generator model including saturation effects", *IEEE Trans. on Power Systems*, Vol. 12, No. 1, pp. 222-229, Feb. 1997.

[8] Bei O., Xiangheng W., Yuguang S., Weijian W. and Weihong W., "Research on the internal faults of the salient-pole synchronous machine", *The Third International IEEE Power Electronics and Motion Control Conference, (PIEMC 2000)*, pp. 558-563, 2000.

[9] Wang X. H., Sun Y. G., Ouyang B., Wang W. J., Zhu Z. Q. and Howe D., "Transient behaviour of salient-pole synchronous machine with internal stator winding faults", *Proc. Inst. Electr. Eng.-Electr. Power Appl.*, Vol. 149, No. 2, pp. 143-151 Mar. 2002.

[10] Kinitsky V. A., "Calculation of internal fault currents in synchronous machine", *IEEE Trans. Power App. Syst.*, Vol. 84, No. 5, pp. 381-389, May 1965.

[11] Lin X., Tian Q., Gao Y. and Liu P., "Studies on the internal fault simulations of a high-voltage cable-wound generator", *IEEE Trans. Energy Convers.*, Vol. 22, No. 2, pp. 240-249, Jun. 2007.

[12] Reichmeider P., Querrey D., Gross C. A., Novosel A. and Salon S., "Partitioning of synchronous machine windings for internal fault analysis", *IEEE Trans. Energy Convers.*, Vol. 15, No. 4, pp. 372-379, Dec. 2000.

- [13] Rahnama M. and Nazarzadeh J., "Synchronous machine modeling and analysis for internal faults detection", *IEEE International Conference on Electric Machines & Drives (IEMDC '07)*, 2007.
- [14] Faiz J. and Pakdelian S., "Diagnosis of static eccentricity in switched reluctance motors based on mutually induced voltages", *IEEE Trans. Energy Convers.*, Vol. 44, No. 8, pp. 2029-204, Aug. 2008.
- [15] Vahedi A. and Behjat V., "Online monitoring of power transformers for detection of internal winding short circuit faults using negative sequence analysis", *European Transactions on Electrical Power*, Vol. 15, Apr. 2010.
- [16] Negrea M. D., "Electromagnetic flux monitoring for detecting faults in electrical machines", *Ph.D.dissertation, Helsinki University of Technology, Laboratory of Electromechanics, Helsinki, Finland, 2007*. The dissertation can be read at <http://lib.tkk.fi/Diss/isbn9512284774>.
- [17] Bui V. P., Chadebec O., Rouve L.-L. and Coulomb J.-L., "Noninvasive fault monitoring of electrical machines by solving the steady-state magnetic inverse problem", *IEEE Trans. Magn.*, Vol. 44, No. 6, pp. 1050-1053, Jun. 2008.
- [18] Joksimovic G. M. and Penman J., "The detection of inter-turn short circuits in the stator windings of operating motors", *IEEE Trans. Ind. Electron.*, Vol. 47, No. 5, pp. 1078-1084, 2000.
- [19] Assaf T., Henao H. and Capolino G. A., "Simplified axial flux spectrum method to detect incipient stator inter-turn short-circuits in induction machine", *IEEE International Symposium on Industrial Electronics*, Vol. 2, pp. 815-819, May 2004.
- [20] Yazidi A., Thailly D., Henao H., Romary R., Capolino G. A. and Brudny J. F., "Detection of stator short-circuit in induction machines using an external leakage flux sensor", *IEEE International Conference on Industrial Technology-ICIT '04*, Hammamet, Tunisia, Vol. 1, pp. 166-169, Dec. 2004.
- [21] Han S. B., Hwang D. H., Yi S. H. and Kang D. S., "Development of Diagnosis Algorithm for Induction Motor Using Flux Sensor", *International Conference on Condition Monitoring and Diagnosis*, Beijing, China, 2008.
- [22] Toni K., Slobodan M. and Aleksandar B., "Detection Of Turn To Turn Faults In Stator Winding With Axial Magnetic Flux In Induction Motors", *IEEE International Conference on Electric Machines & Drives, (IEMDC '07)*, Vol. 1, pp. 826-829, 2007.
- [23] Mirafzal B., Povinelli R. J. and Demerdash N. A. O., "Inter-turn fault diagnosis in induction motors using the pendulous oscillation phenomenon", *IEEE Trans. Energy Convers.*, Vol. 21, No. 4, pp. 871-882, Dec. 2006.
- [24] Nandi S., Toliyat H. A. and Li X., "Condition monitoring and fault diagnosis of electrical machines- A Review", *IEEE Trans. Energy Convers.*, Vol. 20, No. 4, pp. 719-729, Dec. 2005.
- [25] Ranlof M., Perers R. and Lundin U., "On Permeance modeling of large hydrogenerators with application to voltage harmonics prediction", *IEEE Trans. Energy Conversion*, Vol. 25, No. 4, pp. 1179-1186, Dec. 2010.
- [26] Lipo T. A., *Introduction to AC Machine Design*, Power Electronics Research Center, University of Wisconsin, pp. 64-82, 2004.
- [27] Ahmed A. S., Yeh C. C., Demerdash N. A. O. and Mirafzal B., "Analysis of stator winding inter-turn short-circuit faults in induction machines for identification of the faulty phase", *IEEE, Industry Applications Conference, 41st IAS Annual Meeting*, Vol. 3, pp. 1519-1524, Oct. 2006.
- [28] Chan T. F., Wang W. and Lai L. L., "Performance of an axial-flux permanent magnet synchronous generator from 3-D finite-element analysis", *IEEE Trans. Energy Convers.*, Vol. , No. 99, pp. 1-8, 2010.
- [29] Thailly D., Romary R. and Brudny J. F., "Quantitative analysis of the external radial magnetic field for detection of stator inter-turn short-circuit in induction machines", *IEEE, European Conference on Power Electronics and Applications*, 2005.
- [30] Lenz J. and Edelstein A. S., "Magnetic Sensors and Their Applications", *IEEE Sensors Journal*, Vol. 6, No. 3, pp. 631-649, Jun. 2006.
- [31] Tavner P. J., Gaydon B. G. and Ward B. A., "Monitoring generators and large motors", *IEE proceedings*, Vol. 133Pt.B, No. 3, pp.169-180, May 1986.
- [32] Xuan M. T., Simond J. J., Wetter R. and Keller S., "A novel air-gap monitoring system for large low speed hydro-generators", *IEEE, Power Engineering Society General Meeting*, pp. 1-8, 2006.
- [33] Klempner G. and Kerszenbaum I., *Operation and maintenance of large turbo-generators*, John Wiley & Sons Publishers, IEEE Press, the Institute of Electrical and Electronics Engineers, pp. 143-146, 2004.
- [34] Cabanas M. F., Glez F. P., González M. R., Melero M. G., Orcajo G. A., Cano J. M. and Rojas C. H., "A new on-line method for the early detection of broken rotor bars in asynchronous motors working under arbitrary load conditions", *Industry Applications Conference, Fourtieth IAS Annual Meeting*, Vol. 1, pp. 662-669, Oct. 2005.
- [35] Chari M. V. K., "Nonlinear finite element solution of electrical machines under no-load and full-load conditions", *IEEE Trans. Magn.*, Vol. 10, No. 3, pp. 686-689, Sep. 1974.

- [36] Hariri M., Shokouhi S. B. and Mozayani N., "An Improved Fuzzy Neural Network for Solving Uncertainty in Pattern Classification and Identification", *Iranian Journal of Electrical & Electronic Engineering (IJEED)*, Vol. 4, No. 3, pp. 79-93, July 2008.
- [37] Ghods L. and Kalantar M., "Long-Term Peak Demand Forecasting by Using Radial Basis Function Neural Networks", *Iranian Journal of Electrical & Electronic Engineering (IJEED)*, Vol. 6, No. 3, pp. 175-182, Sep. 2010.
- [38] Rajbhandari S., Ghassemlooy Z. and Angelova M., "Performance of the Wavelet Transform-Neural Network Based Receiver for DPIM in Diffuse Indoor Optical Wireless Links in Presence of Artificial Light Interference", *Iranian Journal of Electrical & Electronic Engineering (IJEED)*, Vol. 5, No. 2, pp. 102-111, Jun. 2009.
- [39] Moosavienia A. and Mohammadi K., "A generalized ABFT technique using a fault tolerant neural network", *Iranian Journal of Electrical & Electronic Engineering (IJEED)*, Vol. 1, No. 1, pp. 1-10, Jan. 2005.



**Hamid Yaghobi** was born in Sari, Iran on 1978. He received his B.Sc. degree in Electrical Engineering from K.N.Toosi University of Technology in 2000, Tehran, Iran, M.Sc degree in Electrical Engineering from Ferdowsi University in 2002, Mashhad, Iran and his Ph.D. in electric machinery from the Department of Electrical Engineering of Ferdowsi University, Mashhad, Iran in 2011. His research interests are Electric machinery, Power System Operation and Intelligent Systems.



**Kourosh Ansari** was born in Urmiye, Iran in 1951. He received his B.Sc. and M.Sc. degrees from Tabriz University, Tabriz, Iran, both in Electrical Engineering and his Ph.D. in especially electric machinery from the Department of Electrical Engineering of Jjiang University, Jjiang, China in 1996. He has been an assistant professor of electrical engineering in Ferdowsi University. His research interests are Computational Electromagnetic and Electric machinery.



**Habib Rajabi Mashhadi** was born in Mashhad, Iran in 1967. He received his B.Sc. and M.Sc. degrees with honour from Ferdowsi University of Mashhad, Mashhad, Iran, both in Electrical Engineering and his Ph.D. from the Department of Electrical and Computer Engineering of Tehran University, Tehran, Iran under joint cooperation of Aachen University of Technology, Germany in 2002. He has been an associate professor of electrical engineering in Ferdowsi University. His research interests are Power System Operation and Dynamics, Intelligent Systems and Biological Computation.